TECHNICAL ARTICLE

Improving Arc Joining of Aluminum to Stainless Steel with Pure Al and Al–Cu Twin Hot Filler Wires

Huan He[1,2] · **Mingjie Wang**[1]

Abstract

Tungsten inert gas weld brazing with twin hot wire technique was employed to create sound joints between aluminum alloy and stainless steel using ER1100 and ER2319 filler, respectively. The interfacial intermetallic compound (IMC) consisted of θ-(Fe,Cu)$_4$Al$_{13}$ and minor Cr$_{0.7}$Fe$_{0.3}$Al$_6$, and the precipitate phase in the weld was Al$_2$Cu with ER2319 filler. The interfacial IMC was mainly θ-Fe$_4$Al$_{13}$, and the precipitate phase was FeAl$_6$ with ER1100 filler. The results of mechanical tests suggested that the joint with ER2319 had a higher tensile strength of 283 MPa but more brittle, while the joint with ER1100 exhibited better comprehensive mechanical properties. The joint properties are determined by both interfacial IMCs and precipitate phases in the welded seams. Different ways of controlling the IMCs should be adopted to inhibit the IMC growth by declining the heat input with ER2319 filler and promote the IMC dissolution by adjusting the welding procedures with ER1100 filler.

Keywords TIG weld brazing · Aluminum alloy · Stainless steel · Twin hot wire · Intermetallic

Introduction

Arc weld brazing is an adaptable, convenient, and economical method for joining aluminum/steel dissimilar metals. Nevertheless, it is a challenge to wet the steel surface by molten aluminum, and subsequently difficult to have a stable and uniform appearance. Although some coatings, such as aluminizing, galvanizing [1], and flux [2], and other techniques including the tandem or dual spot laser beam method [3, 4] and hot wire technique [5] can be used to address the wetting difficulty, there are still some issues to be worked out to realize a perfect joint formation of the two dissimilar metals.

Another critical issue to weld brazing of aluminum to steel is the formation of brittle intermetallic compounds (IMCs) at brazing interface due to both chemical reactions and interdiffusion [6], such as orthorhombic η-Al$_5$Fe$_2$ and monoclinic θ-Al$_{13}$Fe$_4$/FeAl$_3$ phases [7]. The presence of the IMCs ensures metallurgical bonding between the aluminum

and steel, but on the other hand, too many brittle IMCs can be detrimental to the properties of joints. Therefore, it is critical to keep the thickness of IMCs in the range of few micrometers to avoid a brittle and easy-to-crack interface.

A variety of solid-state joining methods such as diffusion bonding [8, 9], friction welding [10–12], friction stir welding [13, 14], and friction stir brazing [15] were applied to couple steel with aluminum. Certain solid-state joining processes can minimize or even overcome the problem of IMCs. The joints always have very thin IMCs and satisfactory joint properties due to the low heat input of the solid-state bonding techniques.

However, it is more difficult to suppress the IMCs in electron beam [16], laser [17] and especially the arc weld brazing process [18–21] comparing with the solid-state joining, because the liquid–solid interaction at a high temperature up to 1000 °C generally results in thick IMC layers at the joint interface. Alloying elements, transition layers, and adjustments of heat input have been employed in many studies to limit the formation of brittle IMCs. Aluminum-based fillers or modified brazing fluxes containing alloying elements such as Zn, Si, Mn, Cu, and Ni have been approved to be effective in controlling the thickness and/or structure of IMCs [22–26]. Moreover, transition or insert metals including Zn, Ni, and Cu were also used to inhibit the formation of IMCs [27–29]. In addition, the cold metal transfer (CMT) process

✉ Huan He
  welderhehuan@yahoo.com

1   Department of Mechanical Engineering, Shandong Jiaotong University, Jinan 250023, China

2   Institute of Materials Joining, Shandong University, Jinan 250061, China

[20, 30], a backing block with higher thermal conductivity [31] and a combination of laser welding and roll pressure [32] were developed and applied to suppress the thickness of IMCs. However, no systematic research about the IMC control considering both the brazing fillers and heat input adjustment was reported.

In this work, high-frequency induction heating technique was employed in tungsten inert gas (TIG) weld brazing of aluminum–stainless steel dissimilar metals to preheat twin aluminum fillers and adjust the heat input. The weld appearance, microstructure, and mechanical properties of the joints were analyzed and discussed.

Materials and Methods

The parent materials employed are 3.0-mm-thick 5A06 aluminum alloy and SUS321 stainless steel sheets. The brazing fillers are ER1100 and ER2319 aluminum welding wires with diameters of 1.2 and 1.6 mm. The chemical compositions of the base and filler metals are listed in Table 1. A modified flux ($KAlF_4$ + Al powder) is employed in the experiments. The main ingredients of the modified flux are 10–70 wt.% aluminum powder (with purity of 99.99% and particle size less than 75 μm), non-corrosive flux $KAlF_4$, and 1 wt.% binder potassium sodium tartrate. Employing the modified flux can significantly improve the arc stability and wettability of aluminum brazing fillers [33].

The size of specimen is 100 × 50 mm, with a 45° single-V groove in both steel and aluminum side. The plate surfaces were cleaned by abrasive papers or a scraper and acetone at first, and then, a flux layer, approximately 0.2–0.5 mm thick, was coated on the groove and on both front and back surfaces of the steel in 10 mm width. Butt TIG weld brazing experiments of aluminum to steel were carried out using a standard welding source. The welding parameters were: AC square wave of 100 Hz, 4:1 AC balance, arc length of 3.0–4.0 mm, welding speed of 150 mm^{-min}, and argon gas flow rate of 8–10 L^{-min}.

The twin hot wire equipment based on the high-frequency induction technique in this research consists of induction heating coil, ceramic tube, fixture, and wire guide. The shielding gas is also necessary during the heating process

to protect the wire from oxidation. The schematic of twin wire weld brazing process is illustrated in Fig. 1.

After welding, the joint macrostructure, microstructure, and IMC composition at the interface were examined using an optical microscope, a scanning electron microscope (SEM) and an electron probe micro analyzer (EPMA). Tensile tests were conducted using a INSTRON-5569 testing machine, with a loading speed of 0.5 mm^{-min}. All tests were repeated in triplicate.

Results and Discussion

Heating Effect and Wire Feeding Process

The induction heating hot wire equipment can heat aluminum wire to any expected temperature below 400 °C by adjusting the induction current, when the feeding rate is 1 m^{-min}, as shown in Fig. 2. In this study, the temperatures of the fillers were heated to 350 °C.

High-frequency induction hot wire technique was first proposed by Fan et al. to heat metals with low resistance rate such as aluminum and copper fillers by induction heating instead of the resistance heat in ordinary hot wire methods [34]. Induction heating relies on electrical currents that are induced internally in the materials to be heated. The flow of
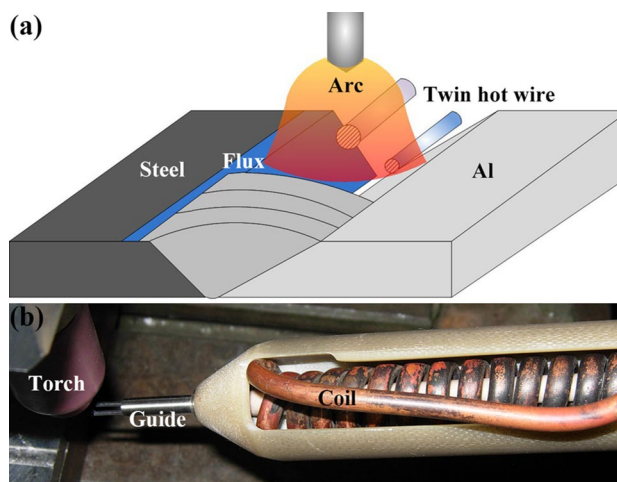

Fig. 1 Schematic of TIG weld brazing process with twin wire

Table 1 Chemical compositions of base and filler metals (wt.%)

Elements	C	Mn	Mg	Al	Si	Cu	Zn	Ti	Ni	Cr	Fe
SUS321	0.12	2	…	…	1	…	…	0.2	8–10	17–19	Bal.
5A06	…	0.5–0.8	5.8–6.8	Bal.	0.4	0.1	0.2	0.1	…	…	0.4
ER1100	…	0.05	…	Bal.	(a)	0.05–0.2	0.1	…	…	…	a
ER2319	…	0.2–0.4	0.02	Bal.	0.2	5.8–6.8	0.1	0.1–0.2	…	…	0.3

aSi plus Fe 0.95
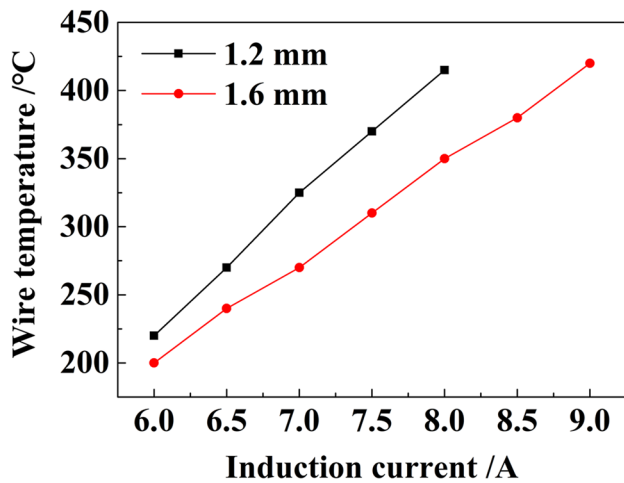
Fig. 2 Heating effect of the twin hot wire system
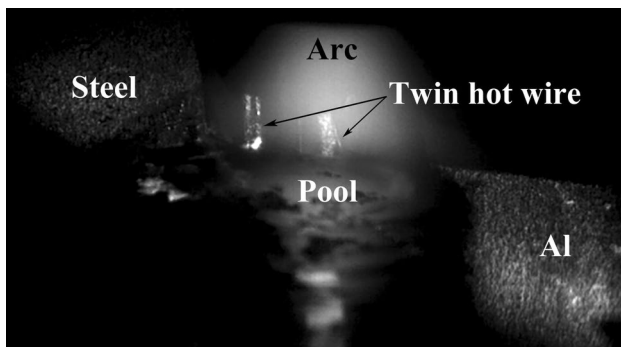
Fig. 3 Feeding process with twin hot wire

Fig. 4 Appearances of the aluminum–steel butt joint (**a**) face appearance and (**b**) back appearance

Table 2 Optimal welding parameters with the two fillers

	Peak current (A)	Pulse on time (%)	Basic current (A)	Average current (A)	Frequency (Hz)
ER2319	130	40	52	83.2	4
ER1100	150	50	70	110	52

AC current through the coil generates an alternating magnetic field which cuts through the workpiece. The alternating magnetic field induces the eddy which can dissipate energy and bring about heating. To heat welding wires, the AC frequency, through its effect on reference depth and efficiency, is one of the important design parameters in induction heating [35]. The AC frequency should high enough for heating a thin wire to an expected temperature.

Based on the hot wire system, the twin hot wire with different diameters was employed to obtain a good formation in the weld brazing process. On the steel side, a filler wire with a 1.6 mm diameter at a relatively higher position can provide sufficient liquid metal for spreading on the face of the weld. On the aluminum side, a wire with a 1.2 mm diameter can easily be melted and fused well together with the base aluminum, as shown in Fig. 3.

The flow of the weld brazing pool is asymmetrical because the two sides of the butt joint have different metals in different states. One side is a solid steel with a layer of flux on its surface, the other side is liquid aluminum melted by the arc. Therefore, when using a single wire, if any fluctuati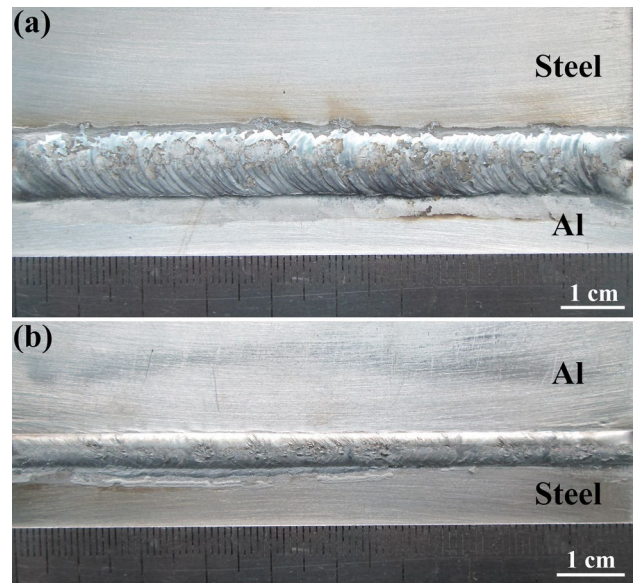on during wire feeding occurs, the pool always flows to one side and leads to a very poor appearance. Twin wire can address this problem and obtain a perfect formation both on the face and the back side, as shown in Fig. 4. Similar application of the twin wire method can be found in variable polarity plasma arc (VPPA) welding and cladding [36, 37].

Welding Procedures

Based on an appropriate experimental design and the following results, considering both the weld appearance and joint strength, the optimal welding parameters with the two different fillers were obtained. As illustrated in Table 2, the average welding current with employing ER2319 filler was 83.2 A, which was the minimum welding current to ensure a satisfactory face and back formation, while the average welding current with using ER1100 filler was up to 110 A, a relatively high value. It needs to be emphasized, if the average welding current is lower than 83 A or higher than 120 A, welding defects such as lack of fusion, incomplete penetration, undercutting, and burn through will occur.

Microstructure Analysis

The SEM images and EPMA results of the interfaces with the different fillers are shown in Fig. 5 and Table 3, respectively. Although the thicknesses of the IMCs are similar to the two kinds of fillers, there are some differences of element composition in the IMCs. With the ER1100 filler, the IMC is Fe_4Al_{13} with solid solution elements of Cr and Ni, and a significant difference using the ER2319 compared with ER1100 is the existence of Cu in the IMC. Besides, there is another phase in the vicinity of the IMC around the interface, as shown in Fig. 5d. The phase with the homogeneity range 86.3–87.6 at.% Al has a composition closer to Cr_2Al_{13}, $CrAl_6$, or $CrAl_7$ [38]. In the presence of a third metal (Fe, Mn, etc.), the $CrAl_6$ phase is known to give rise to another phase with fivefold symmetry whose composition corresponds to the chemical formula $Cr_{0.7}Fe_{0.3}Al_6$ [39]. Similar phases were observed by the interaction of iron–chromium alloys with liquid aluminum [40].

Moreover, the microstructures in the welded seams are distinct from each other. The phases in the welded seams with employing ER1100 and ER2319 are Al_6Fe and Al_2Cu, respectively, according to the previous studies [22, 26]. The phase $FeAl_6$ has an orthorhombic unit cell with $a = 0.646$ nm, $b = 0.744$ nm, $c = 0.878$ nm [41, 42]. The metastable compound $FeAl_6$ has also been found in rapidly chilled alloys, aged aluminum alloys, and interface formed

**Table 3** EPMA analysis results of IMCs in interfaces, at.%

	Al	Fe	Cr	Ni	Cu
ER1100	76.09	19.71	3.03	1.17	…
ER2319	75.81	17.41	3.49	1.28	2.01
	87.05	4.09	6.93	0.45	1.79

by interaction of iron–chromium alloy and liquid aluminum [40, 43]. The phase Al_2Cu shows a I4/mcm structure with $a = 0.607$ nm and $c = 0.487$ nm [44].

Mechanical Property and Fracture Behavior

As can be seen in Fig. 6, the tensile strengths of the joints with employing ER2319 and ER1100 are 283 MPa and 234 MPa, respectively, which are much more superior than the 175 MPa with ER2319 [45] and the 170 MPa with ER1100 filler [33] in the previous studies. The overall strength is greater than that of the filler material, partly because the joints have reinforcements. In addition, the diffused elements from the steel to aluminum also can strengthen the joints.

The fracture positions of the joints with the two kinds of fillers were different. With employing the ER1100 filler, it mainly fractured at the brazing side and the crack was derived from steel–IMC or IMC–seam interface, as
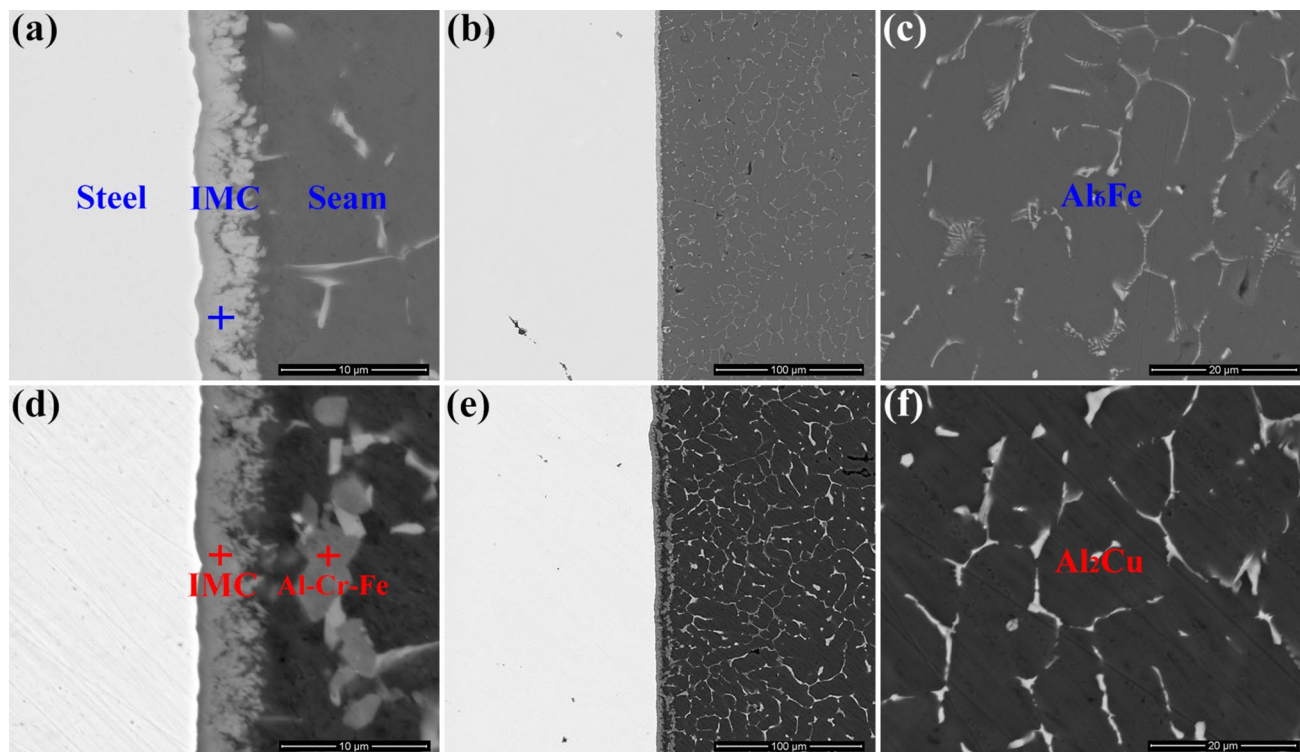
Fig. 5 SEM images of the joints (**a**–**c**) with ER1100 filler and (**d**–**f**) with ER2319 filler
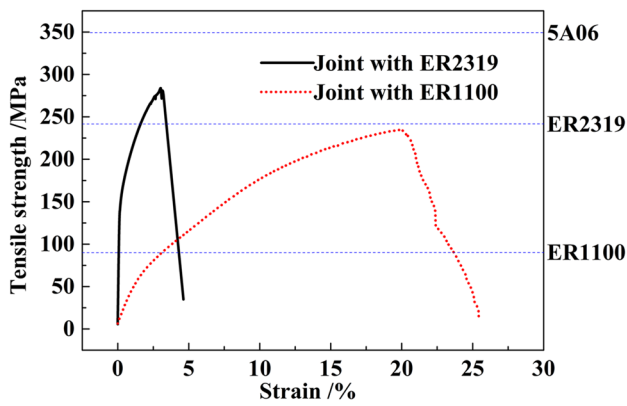
Fig. 6 Stress–strain plots of aluminum–steel butt joints with different fillers

shown in Fig. 7a and c. While with the ER2319, fracture occurred at the welded seam in the aluminum fusion side and the crack developed along the Al$_2$Cu phase, as shown in Fig. 7b and d. The joint filled by ER2319 was much more brittle than ER1100.

Relationship Between Welding Procedure, Microstructures, and Mechanical Behaviors

Compared with using the wire of room temperature, the application of the hot wire at 350 °C to join aluminum and steel can decrease the machine welding current setting from 100 to 83 A and furthermore lower the heat input of welding arc to the brazing interface. It is critical to reduce the IMC thickness by lowering the heat input with ER2319 filler. In addition, if the welding current is fixed, employing the hot wire can improve the pool temperature, which is effective in affecting the IMC and joint properties with ER1100 filler.

The thickness of an IMC is governed by specific alloying elements, reaction time, and temperature. Both of these factors are different for the two joints with different fillers (composition and process parameters). The mechanisms of the interface reactions with the two fillers are different. The processes of growth of a compound layer at the solid–liquid interface and its dissolution into the liquid phase take place simultaneously. By increasing the rate of dissolution, it is possible to significantly reduce the thickness of the IMC layer [46]. For the joint with ER2319 filler, the IMC is
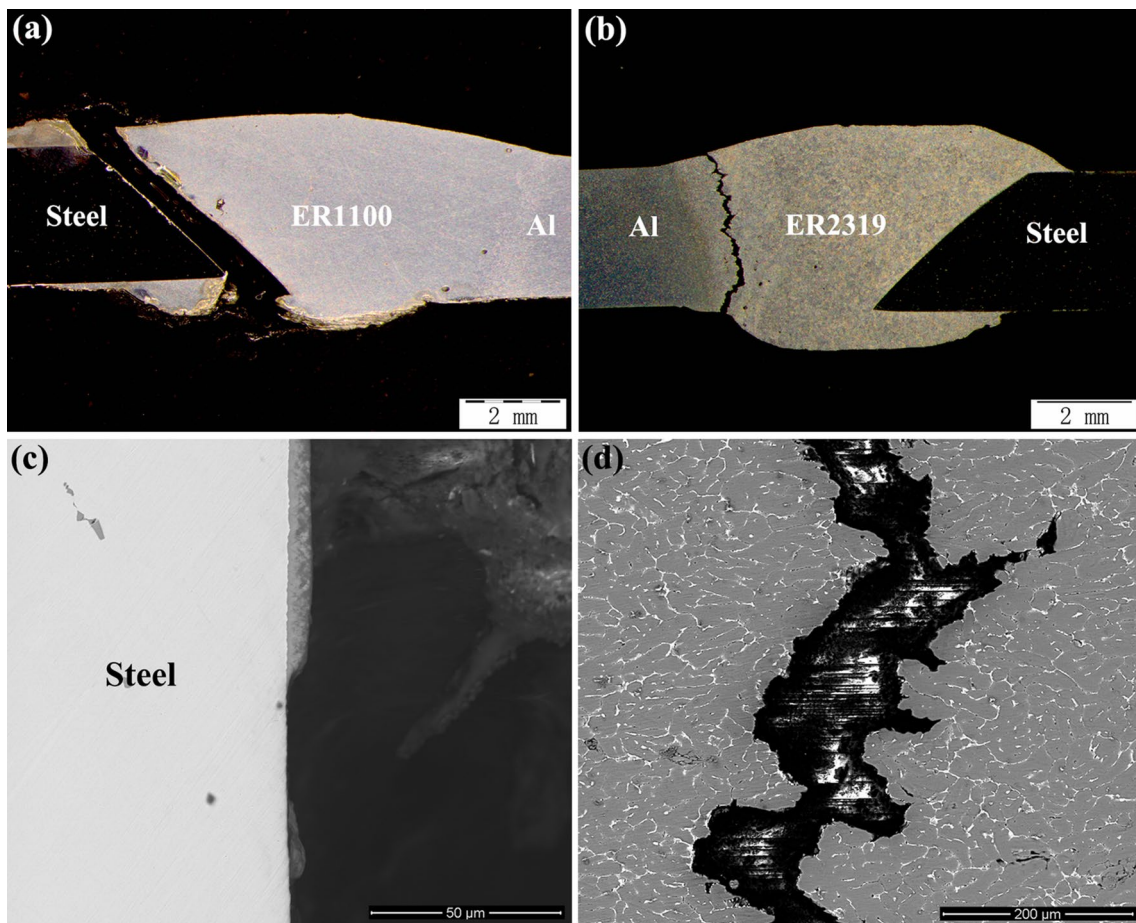
Fig. 7 Fracture modes of the joints (**a**, **c**) with ER1100 filler and (**b**, **d**) with ER2319 filler

Fe_4Al_{13} and the microstructure in the welded seam is Al_2Cu. The formation of Al_2Cu cannot consume the Fe atom and promote the dissolution of IMC. Therefore, controlling the IMC growth by decreasing the heat input is the only effective way to reduce the IMC thickness. Considering the joint with ER1100 filler, the IMC is Fe_4Al_{13} and the phase in the welded seam is Al_6Fe. The formation of the $FeAl_6$ can consume the Fe atom and then promote the dissolution of the Fe_4Al_{13} into the liquid aluminum. Thus, if the dissolution rate exceeds the growth rate of IMC under certain welding conditions, the IMC thickness will be suppressed.

The joint properties are affected by both IMC and microstructure in the welded seam. The thickness of IMC is always an important factor that influences the mechanical properties. It has been described that joint strength increases with reaction layer thickness decreasing [47]. However, there is no significant difference on IMC thickness between the two interfaces with the two different fillers; therefore, the IMC thickness is not a key factor that influences the properties in this study. Alloying element also affects the properties of IMCs and then the joints. Some contents of Cu atoms replacing Fe in $Al_{13}Fe_4$ can reduce its hardness significantly [22], which contributes to the improvement in the interface strength. Besides, the effect of the Al–Cr–Fe phase near the IMC on the joint property with ER2319 is not very clear. The information only can be obtained is the Vickers hardness of the Al–Cr phase is 510–714 HV, while the hardness of $FeAl_3$ is 816–1020 HV [48].

Strength phases in the welded seams mentioned above also determine the joint strength. With the ER2319 welding wire, a lot of copper was available for precipitation reaction and the Al_2Cu phase can be abundantly formed, causing higher tensile strength compared with the ER1100 welding wire. Although the Al_2Cu can strengthen the seam effectively, it decreases the toughness of the joint as well [48]. With employing ER1100 filler, the thickness of IMC is also small enough and the welded seam has adequate strength and toughness because of the existence of Al_6Fe. Hence, the joint has the best comprehensive mechanical properties.

Conclusions

High-frequency induction twin hot wire technique was successfully developed in TIG weld brazing of aluminum–stainless steel dissimilar metals with ER2319 and ER1100 fillers, respectively.

With ER2319 filler, the interfacial IMC consisted of θ-$(Fe,Cu)_4Al_{13}$ chiefly and minor $Cr_{0.7}Fe_{0.3}Al_6$, of which the phase in the weld was identified as Al_2Cu. With ER1100 filler, the main ingredient of interfacial IMC was θ-Fe_4Al_{13}, and the microstructure in the weld was identified as $FeAl_6$.

The tensile strengths of the joints with using ER2319 and ER1100 fillers are 283 and 234 MPa, respectively. The joint with ER2319 is much more brittle than ER1100. The joint properties are affected by both IMC and microstructure in the welded seam.

The growth of a compound layer at the solid–liquid interface and its dissolution into the liquid phase take place simultaneously. For the joint with ER2319 filler, controlling the IMC growth by decreasing the heat input is effective, as there is neither chemical reaction to promote the dissolution of IMCs nor decomposition reaction from IMCs to Al_2Cu. With ER1100 filler, the formation of the $FeAl_6$ can promote the dissolution of the Fe_4Al_{13} into the liquid aluminum and then reduce the IMC thickness.

References

1. H. Zhang, J. Liu, Microstructure characteristics and mechanical property of aluminium alloy/stainless steel lap joints fabricated by MIG weld brazing process. Mater. Sci. Eng., A **528**(19–20), 6179–6185 (2011)
2. J.L. Song, S.B. Lin, C.L. Yang, G.C. Ma, H. Liu, Spreading behavior and microstructure characteristics of dissimilar metals TIG weld brazing of aluminum alloy to stainless steel. Mater. Sci. Eng., A **509**(1–2), 31–40 (2009)
3. K. Saida, H. Ohnishi, K. Nishimoto, Fluxless laser brazing of aluminium alloy to galvanized steel using a tandem beam-dissimilar laser brazing of aluminium alloy and steels. Weld. Int. **24**(3), 161–168 (2010)
4. H. Laukant, C. Wallmann, M. Korte, U. Glatzel, Flux-less joining technique of aluminium with zinc-coated steel sheets by a dual-spot-laser beam. Adv. Mater. Res. **6–8**, 163–170 (2005)
5. A. Mathieu, S. Pontevicci, J. Viala, E. Cicala, S. Matte, D. Grevey, Laser brazing of a steel/aluminium assembly with hot filler wire (88% Al, 12% Si). Mater. Sci. Eng., A **435–436**, 19–28 (2006)
6. L. Agudo, D. Eyidi, C.H. Schmaranzer, E. Arenholz, N. Jank, J. Bruckner, A.R. Pyzalla, Intermetallic Fe_xAl_y-phases in a steel/Al-alloy fusion weld. J. Mater. Sci. **42**(12), 4205–4214 (2007)
7. X. Li, A. Scherf, M. Heilmaier, F. Stein, The Al-rich part of the Fe–Al phase diagram. J. Phase Equilibria Diffus. **37**(2), 162–173 (2016)
8. E.R. Naimon, J.H. Doyle, C.R. Rice, D. Vigil, D.R. Walmsley, Diffusion welding of aluminum to stainless-steel. Weld. J. **60**(11), 17–20 (1981)
9. J.H. Kong, M. Okumiya, Y. Tsunekawa, K.Y. Yun, S.G. Kim, M. Yoshida, A novel bonding method of pure aluminum and SUS304 stainless steel using barrel nitriding. Metall. Mater. Trans. A **45**(10), 4443–4453 (2014)
10. M.B. Uday, M.N. Ahmad Fauzi, H. Zuhailawati, A.B. Ismail, Advances in friction welding process: a review. Sci. Technol. Weld. Join. **15**(7), 534–558 (2010)
11. W. Li, A. Vairis, M. Preuss, T. Ma, Linear and rotary friction welding review. Int. Mater. Rev. **61**(2), 71–100 (2016)

12. T. Debroy, H.K.D.H. Bhadeshia, Friction stir welding of dissimilar alloys—a perspective. Sci. Technol. Weld. Join. **15**(4), 266–270 (2010)

13. M. Reddy, S. Rao, T. Mohandas, Role of electroplated interlayer in continuous drive friction welding of AA6061 to AISI 304 dissimilar metals. Sci. Technol. Weld. Join. **13**(7), 619–628 (2018)

14. A. Simar, M.-N. Avettand-Fènoël, State of the art about dissimilar metal friction stir welding. Sci. Technol. Weld. Join. **22**(5), 389–403 (2016)

15. G. Zhang, W. Su, J. Zhang, Z. Wei, Friction stir brazing: a novel process for fabricating Al/Steel layered composite and for dissimilar joining of Al to steel. Metall. Mater. Trans. A **42**(9), 2850–2861 (2011)

16. F.W. Bach, A. Beniyash, K. Lau, R. Versemann, Joining of steel-aluminium hybrid structures with electron beam on atmosphere. Adv. Mater. Res. **6**, 143–150 (2005)

17. P. Wang, X. Chen, Q. Pan, B. Madigan, J. Long, Laser welding dissimilar materials of aluminum to steel: an overview. Int. J. Adv. Manuf. Technol. **87**(9), 3081–3090 (2016)

18. Y. Zhang, J. Huang, Z. Cheng, Z. Ye, H. Chi, L. Peng, S. Chen, Study on MIG–TIG double-sided arc weld brazing of aluminum and stainless steel. Mater. Lett. **172**, 146–148 (2016)

19. Y. Shi, G. Zhang, Y. Huang, L. Lu, J. Huang, Y. Shao, Pulsed double-electrode GMAW-brazing for joining of aluminum to steel. Weld. J. **93**(6), 216–224 (2014)

20. S. Madhavan, M. Kamaraj, L. Vijayaraghavan, Microstructure and mechanical properties of cold metal transfer welded aluminium/dual phase steel. Sci. Technol. Weld. Join. **21**(3), 194–200 (2016)

21. A. Das, M. Shome, S.F. Goecke, A. De, Numerical modelling of gas metal arc joining of aluminium alloy and galvanised steels in lap joint configuration. Sci. Technol. Weld. Join. **21**(4), 303–309 (2016)

22. S. Lin, J. Song, C. Yang, C. Fan, D. Zhang, Brazability of dissimilar metals tungsten inert gas butt weld brazing between aluminum alloy and stainless steel with Al–Cu filler metal. Mater. Des. **31**(5), 2637–2642 (2010)

23. J. Yang, Y. Li, H. Zhang, W. Guo, Y. Zhou, Control of interfacial intermetallic compounds in Fe–Al joining by Zn addition. Mater. Sci. Eng., A **645**, 323–327 (2015)

24. Y. Su, X. Hua, Y. Wu, Influence of alloy elements on microstructure and mechanical property of aluminum–steel lap joint made by gas metal arc welding. J. Mater. Process. Technol. **214**(4), 750–755 (2014)

25. L.A. Jácome, S. Weber, A. Leitner, E. Arenholz, J. Bruckner, H. Hackl, A.R. Pyzalla, Influence of filler composition on the microstructure and mechanical properties of steel–aluminum joints produced by metal arc joining. Adv. Eng. Mater. **11**(5), 350–358 (2009)

26. H. He, S. Lin, C. Yang, C. Fan, Z. Chen, Combination effects of Nocolok flux with Ni powder on properties and microstructures of aluminum–stainless steel TIG weld brazing joint. J. Mater. Eng. Perform. **22**(11), 3315–3323 (2013)

27. H. Springer, A. Szczepaniak, D. Raabe, On the role of zinc on the formation and growth of intermetallic phases during interdiffusion between steel and aluminium alloys. Acta Mater. **96**, 203–211 (2015)

28. S. Chen, J. Huang, K. Ma, X. Zhao, A. Vivek, Microstructures and mechanical properties of laser penetration welding joint with/without Ni-foil in an overlap steel-on-aluminum configuration. Metall. Mater. Trans. A **45**(7), 3064–3073 (2014)

29. S. Chen, Z. Zhai, J. Huang, X. Zhao, J. Xiong, Interface microstructure and fracture behavior of single/dual-beam laser welded steel–Al dissimilar joint produced with copper interlayer. Int. J. Adv. Manuf. Technol. **82**(1–4), 631–643 (2016)

30. B. Mezrag, F. Deschaux-Beaume, M. Benachour, Control of mass and heat transfer for steel/aluminium joining using cold metal transfer process. Sci. Technol. Weld. Join. **20**(3), 189–198 (2015)

31. R. Borrisutthekul, T. Yachi, Y. Miyashita, Y. Mutoh, Suppression of intermetallic reaction layer formation by controlling heat flow in dissimilar joining of steel and aluminum alloy. Mater. Sci. Eng., A **467**(1–2), 108–113 (2007)

32. M. Rathod, M. Kutsuna, Joining of aluminum alloy 5052 and low-carbon steel by laser roll welding. Weld. J. **83**(1), 16–26 (2004)

33. H. He, C. Yang, S. Lin, C. Fan, Z. Chen, Z. Chen, Flux modification for AC–TIG braze welding of aluminium to stainless steel. Sci. Technol. Weld. Join. **19**(6), 527–533 (2014)

34. C.L. Fan, Y.C. Liang, C.L. Yang, Y.P. Zhu, High frequency induction hot wire TIG welding of aluminum alloy. Trans. China Weld. Inst. **27**(7), 49–52 (2006)

35. S. Zinn, S.L. Semiatin, *Elements of Induction Heating: Design, Control, and Applications* (ASM International, Metals Park, OH, 1988)

36. J. Li, *Research on Technology of Variable Polarity Plasma Arc Welding with Twin-Wire Filler* (Harbin Institute of Technology, Harbin, 2009)

37. Z. Sun, M. Kuo, D. Pan, Twin wire gas tungsten arc cladding. SIMTech Technical Report (PT/99/004/JT) (1999)

38. J.L. Murray, The Al–Cr (aluminum–chromium) system. J. Phase Equilib. **19**(4), 367–375 (1998)

39. F. Woude, P.J. Schurer, A study of quasi-crystalline Al–Fe alloys by Mössbauer-effect spectroscopy and diffraction techniques. Can. J. Phys. **65**(10), 1301–1308 (1987)

40. K. Barmak, V. Dybkov, Interaction of iron–chromium alloys containing 10 and 25 mass% chromium with liquid aluminium part II formation of intermetallic compounds. J. Mater. Sci. **39**(13), 4219–4230 (2004)

41. L. Walford, The structure of the intermetallic phase $FeAl_6$. Acta Crystallogr. **18**(2), 287–291 (1965)

42. A.A. Putyatin, V.E. Davydov, S.N. Nesterenko, High temperature interactions in the Fe–Al–C system at 6 GPa pressure. J. Alloy. Compd. **179**(1–2), 165–175 (1992)

43. L.F. Mondolfo, *Aluminum Alloys: Structure and Properties* (Butterworths London, Boston, 1976)

44. S.C. Wang, M.J. Starink, Precipitates and intermetallic phases in precipitation hardening Al–Cu–Mg–(Li) based alloys. Int. Mater. Rev. **50**(4), 193–215 (2005)

45. J. Song, S. Lin, C. Yang, C. Fan, G. Ma, Analysis of intermetallic layer in dissimilar TIG weld brazing butt joint of aluminium alloy to stainless steel. Sci. Technol. Weld. Join. **15**(3), 213–218 (2010)

46. V.I. Dybkov, *Solid State Reaction Kinetics* (IPMS publications, Kyiv, 2013)

47. H. Springer, A. Kostka, J. Dos Santos, D. Raabe, Influence of intermetallic phases and Kirkendall-porosity on the mechanical properties of joints between steel and aluminium alloys. Mater. Sci. Eng., A **528**(13–14), 4630–4642 (2011)

48. V.S. Zolotorevsky, N.A. Belov, M.V. Glazoff, *Casting Aluminum Alloys* (Elsevier Science, Amsterdam, 2007)